COMPUTATION FLUID DYNAMICS OF HEAT TRANSFER ENHANCEMENT IN RECTANGULAR DUCT USING PROTRUSIONS PASSIVE TECHNIQUE

Supported by tetfund TERTIARY EDUCATION TRUST FUND

Aasa S.A.[1*] Shote A.S.[1] and Adio S.A.[2]
[1]Department of Mechanical Engineering, Olabisi Onabanjo University, Ibogun Campus, Ago-Iwoye, Ogun State, Nigeria
[2]Department of Mechanical, Obafemi Awolowo University, Ile-Ife, Nigeria
Corresponding Author: aasa.samson@oouagoiwoye.edu.ng*

Received: August 15, 2023 Accepted: December 28, 2023

Abstract: Heat transfer and fluid flow characteristics were computationally studied using passive oval protrusion, (POP), in a rectangular channel. The study employed rectangular computational domain of length 500 mm and width 170 mm for both smooth and roughened surface profiles. The simulations are carried out in three different aspect ratios corresponding to height of 5, 7 and 10 mm under a constant wall heat flux and for Reynolds numbers Re = 600, 1,000, 5,000, 7,000, 12000 and 15,000 in a rectangular duct. Having acquire the computational domain, the mesh integrity tests were carried using four different mesh sizes after which mesh size of 1.5 million cells were selected. The flow heat transfer and pressure drop characteristic was simulated using Star CCM+ using the (k-omega) turbulence model. One side of the for walls are embellished with POP, these combined oval geometry protrusions are fixed on the top wall of the channel. Baseline results are validated for both friction factors and Nusselt numbers using Shah and London and Dittus Boelter correlations respectively. The results of temperature and pressure drop distributions along the mainstream channel are acquired analyze for the smooth and roughened surface are averaged and compared experiments ones. An enhancement in the rate of heat transfer was observed in the channel and an increase in heat transfer is observed as aspect ratio decreases, same trend is observed for friction factors. An optimum heat transfer effect of 14.3 % compared to the smooth case is noticed.

Keywords: Heat Enhancement, passive technique, Pressure drop penalty, Protrusion, Nusselt Number, Rectangular Duct, and Thermal Performance.

Introduction

Passive Oval Protrusion (POP) is a surface modification technique that has been shown to be effective in enhancing heat transfer in a variety of applications. The technique involves creating a series of small, oval-shaped protrusions on the surface of an object in a pattern that enhances heat transfer from the surface to the surrounding fluid or environment. The design of POP creates a tempestuous flow over the surface of the object, increasing the rate of heat transfer and improving the overall efficiency of the system.
Heat transfer is a critical process that plays a crucial role in many industries, such as aerospace, automotive, electronics, energy, packaging, and process industry. Efficient heat transfer is essential to ensure the proper functioning and longevity of equipment and systems. Conventional methods of heat transfer, such as conduction and convection, have limitations and may not be sufficient to meet the increasing demands of modern technology. Therefore, researchers are continually exploring new and innovative ways to enhance heat transfer.

Among various surface modification techniques, the use of POP has gained considerable attention due to its simplicity and effectiveness. The technique was first proposed by Kline and McClintock in 1953, who observed that the flow over a flat plate could be significantly altered by the presence of small, elliptical-shaped bumps on the surface (Kline & McClintock, 1953).

Since then, several studies have been conducted to investigate the effectiveness of POP in enhancing heat transfer. One of the earliest studies on POP was conducted by Chang and Yang (1988), who investigated the effect of protrusion geometry on heat transfer enhancement in a turbulent boundary layer. The researchers found that the size and shape of the protrusions had a significant effect on the heat transfer enhancement. They also found that the heat transfer enhancement increased with increasing protrusion height and Reynolds number. Several other studies have also investigated the effectiveness of POP in different applications. For example, Inada et al. (2013) studied the effect of POP on the performance of a finned-tube heat exchanger. The researchers found that the use of POP increased the heat transfer coefficient by up to 90%, leading to a significant improvement in the heat exchanger's efficiency. Similar results were obtained by Kim et al. (2017), who studied the effect of POP on a tube bank heat exchanger. The researchers found that the use of POP increased the heat transfer coefficient by up to 100%, leading to a significant improvement in the heat exchanger's efficiency.

POP has also been shown to be effective in electronic cooling applications. For example, Lee et al. (2011) investigated the effect of POP on the cooling performance of a microchannel heat sink. The researchers found that the use of POP reduced the temperature of the electronic components by up to 20%, improving their reliability and longevity. Similarly, Koyama et al. (2013) studied the effect of POP on the cooling performance of a laptop computer. The researchers found that the use of POP reduced the

temperature of the laptop by up to 6°C, improving its performance and reliability.

The effectiveness of POP depends on several factors, including the size and shape of the protrusions, the pattern in which they are arranged, and the Reynolds number of the fluid or air flowing over the surface. Reynolds number is a dimensionless quantity that describes the flow regime of a fluid or gas. At low Reynolds numbers, the flow is typically laminar, while at high Reynolds numbers, the flow becomes turbulent. POP is most effective in the turbulent flow regime, where the vortices created by the protrusions are amplified, leading to a significant increase in heat transfer.

Despite its effectiveness, POP also has some limitations. One of the significant limitations of POP is that it is a passive technique, meaning that it cannot be turned on or off. Once the protrusions are in place, they generate high pressures penalty especially when the protrusion gets extreme in the flow areas. The need for better strategies to keep the positive effect of protrusion with low pressure penalties has prompted the combined POP arrangement in this. Therefore this studies focuses on combined effect of POP on the performance of system in a rectangular duct.

Methodology

Geometry

The geometry was created using Solidworks Rx 2015 and saved as a parasolid file (x.t extension) before it's imported into the simulation software. The passive oval protrusions inline arrangement is considered in the present work, the geometry of different channel height of 5mm, 7mm and 10mm of this arrangement is studied for its heat and flow characteristics. The geometry consists of an inlet, outlet and wall boundaries. The channel width and length are 170 mm and 500 mm respectively, and protrusions are arranged on the top wall with a width of 10 mm and length 20 mm. The protrusions are compound arrangement of two oval geometry that form V-shape which are made to be at angle 45 degree to mainstream. The details of POP top endwall is presented in figure 2.1 and table 2.1 explains the parameters.

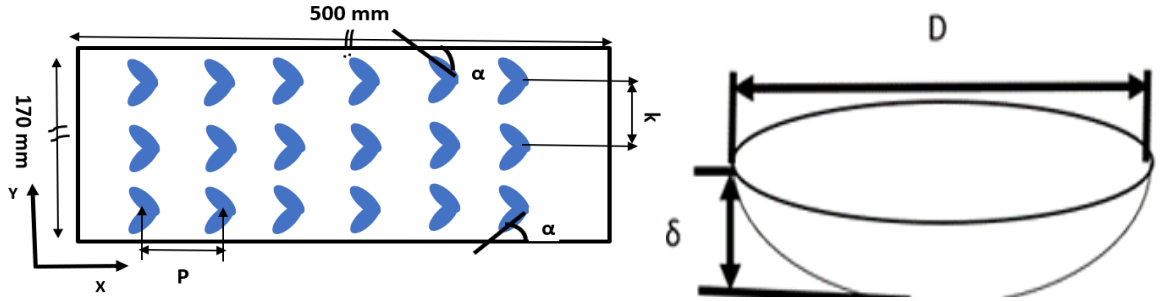

Figure 2.1: Domain model with inline arrangement protrusions and protrusion details

Table 2. 1: Test parameters

#	LXB (mm)	Pitch (P/mm)	K (mm)	D (mm)	δ (mm)	α (degree)	H (mm)
1.	170 x 500	30	15	20	10	45	5
2.	170 x 500	30	15	20	10	45	7
3.	170 x 500	30	15	20	10	45	10

Computational methodology

Having perform the model design in Solidworks and three-dimensional simulation is then performed to simulate the fluid flow and heat transfer behaviour in the smooth and protruded domain model. The simulation software, STAR CCM+, is used to numerically solve the equations, which are the equations of continuity for conservation of mass, Navier-Stokes equation for conservation of momentum and energy equation. These general assumptions considered in the analysis are as follows: The heat transfer and fluid flow are steady, three dimensional, turbulent, fully developed and the fluid flow is compressible. The flow is single phase across the channel. The convective fluid (air) is considered temperature dependent, and the thermodynamic properties is constant. The effect of heat loss through radiation are assumed to be negligible. The wall of the channel and the material of the ribs are homogenous and isotropic.

Computational Solution Domain in this present numerical study of a rectangular channel with roughened wall of a POP is simulated. The three-dimensional analysis as adopted, and the results are compared with the existing experimental results of same protrusions. The domain consists of three sections- entry section, test section and end section which are 500mm long. The entry section is to fully develop and straighten the fluid flow and the end section is to control the end effect in the test section. Boundary conditions the inlet air flow velocity is set at the range of 4 to 8 m/s with the outlet given pressure boundary condition at atmospheric pressure. The top-protruded endwall of the study domain is kept at constant heat flux, all other walls are kept at adiabatic conditions. The working fluid in all cases is taken as air and the channel material is taken as polycarbonate. The internal air temperature in the channel is 300 K and no-slip boundary condition is given along the wall.

Governing Equations

In this study the single-phase flow model has been used to solve the respective category problems. It is important to set the governing equations for the three-dimensional steady flow which are the standard continuity equation for

conservation of mass, Navier Stokes equation for conservation of momentum and energy equations for predicting the conjugate heat transfer Aasa et al (2021),

2.2.2 Standard k- omega model

***Continuity equation*:**

$$\frac{\partial}{\partial x}(\rho Ui) = 0 \qquad (2.1)$$

Where ρ and Ui is the density and flow velocity of the fluid

2.2.4 Momentum equation:

$$\frac{\partial(\rho u_i u_j)}{\partial x_i} = \frac{\partial p}{\partial x_i} + \frac{\partial}{\partial x_j}\left[\mu\left(\frac{\partial u_i}{\partial x_i} + \frac{\partial u_j}{\partial x_j}\right)\right] + \frac{\partial}{\partial x_j}\left(-\rho\overline{u_i u_j}\right) \qquad (2.2)$$

Energy equation:

$$\frac{\partial}{\partial x_j}(\rho u_i T) = \frac{\partial}{\partial x_j}\left[(\Gamma + \Gamma_t)\frac{\partial T}{\partial x_j}\right] \qquad (2.3)$$

Where Γ and Γi are molecular thermal diffusivity and turbulent thermal diffusivity respectively and are given by;

$$\Gamma = \frac{\mu}{P_r}, \Gamma_t = \frac{\mu_t}{P_{rt}} \qquad (2.4)$$

The turbulent viscosity term μ_t is given as

$$\mu_t = \rho C_\mu \frac{k^2}{\ell} \qquad (2.4.1)$$

The equations 2 and 4 are called Reynolds Averaged Navier-Stokes equation (RANS). The additional term in the momentum equation $\left(-\rho\overline{u_i u_j}\right)$ is called Reynolds stress and is used for collecting the effects of turbulence. In other to get a closed form of equation of the Reynolds stress, a common way to achieve this is to use Boussinesq Hypothesis to relate the Reynold stress to mean velocity gradient as given below:

$$\left(-\rho\overline{u_i u_j}\right) = \mu_t\left(\frac{\partial u_i}{\partial x_i} + \frac{\partial u_j}{\partial x_j}\right) \qquad (2.5)$$

Renormalized Group (RNG) k-ε turbulence model

To attain accurate prediction in the ribbed channel, the standard k-ε turbulence model, and the Renormalized Group (RNG) k-ε turbulence model were selected by implementing the Boussinesq hypothesis:

$$\frac{\partial}{\partial x_i}(\rho k u_i) = \frac{\partial p}{\partial x_j}\left(\alpha_k \mu_{eff}\frac{\partial k}{\partial x_j}\right) + G_k - \rho\varepsilon \qquad (2.6)$$

$$\frac{\partial}{\partial x_i}(\rho\varepsilon u_i) = \frac{\partial p}{\partial x_j}\left(\alpha_\varepsilon \mu_{eff}\frac{\partial z}{\partial x_j}\right) + C_{1z}G_k\frac{z}{k} - C_{2z}\rho\frac{z^2}{k} - R \qquad (2.7)$$

The governing equations in the rectangular Cartesian coordinate system (the continuity, conservation of momentum and energy equations used to solve the forced turbulent fluid flow and heat transfer) can be written as follows: Saha and Acharya (2014)

From the equation (2.6) and (2.7), the parameters: μ_{eff} is the effective turbulent viscosity, μ_i is the turbulent viscosity respectively and is given by:

$$\mu_{eff} = \mu + \mu_z \qquad (2.8)$$

$$\mu_z = \rho C_\mu \frac{k^z}{z} + \mu_z \qquad (2.9)$$

G_k represents the generation of turbulence kinetic energy due to the mean velocity gradients and it relation to the Reynolds stress is given by:

$$G_k = -\rho\overline{u_i u_j}\frac{\partial u_j}{\partial x_i} \qquad (2.10)$$

$C_{1\varepsilon}$, $C_{2\varepsilon}$, C_μ, α_k and α_ε are constants and their values are 1.42, 1.68, 0.0845, 1.39 and 1.39 respectively.

To attain accurate prediction of the heat and hydraulic characteristic of the protruded channel, the selected standard k-ε model and the Renormalized Group (RNG) k-ε model results is compared with Dittus-Boelter empirical correlation for Nusselts number for smooth channel, given below:

$$Nu_s = 0.023\mathrm{Re}^{0.8}\,\mathrm{Pr}^{0.4} \qquad (2.11)$$

It has been observed that this present study the RNG k-ε model is in good agreement with Dittus-Boelter empirical correlation results and has been employed to simulate the flow and heat transfer in the channel.

The artificially roughen wall of the channel with inclined protrusions with feather-like shape results enhancement in heat transfer, which is predicted by calculating the Nusselts number for the roughened rectangular channel. The heat transfer enhancement is also accompanied by an increase in friction factor which is computed as

$$Nu_s = \frac{Q_c \times D_h}{L \times B \times k_a(T_w - T_i)} \qquad (2.12)$$

The average friction factor for the flow in the roughened channel is given by

$$f = \frac{\Delta p \times D_h}{2 \times \rho \times l \times v^2} \qquad (2.13)$$

The Reynolds number of fluid flow is expressed as

$$\mathrm{Re} = \frac{\rho u D_h}{\mu} \qquad (2.14)$$

To consider the thermal performance and hydraulic effect together in order to get the thermo-hydraulic performance, the thermos-hydraulic efficiency can be calculated. It is defined as:

$$\eta_{THPP} = \frac{Nu_r / Nu_s}{\left(f_r / f_s\right)^{1/3}} \quad (2.15)$$

Where Nu is the Nusselts number and f is the friction factor. The subscript r and s represent rough and smooth channel.
The friction factor and Nusselts number for the smooth surface channel is validated from Blasius equation, Shah and London (1978), Karma Nikuradse equation (Crawford and London, 1993) and Dittus-Boelter equation (1998).

$$f = 2(2.23InRe - 4.639)^2 \quad (2.16)$$

$$f = \frac{24((1-1.3553\alpha_c)+(1.9467\alpha_c{}^2)-(1.7012\alpha_c{}^3)+(0.9564\alpha_c{}^4)-(0.2537\alpha_c{}^5))}{Re} \quad (2.17)$$

Geometry Meshing and Grid Generation

Under the assumption of fully developed flow and heat transfer, it is better to choose the smallest repetitive unit as the computational domain to minimize the computational tine, cost and should be capable of capturing all the relevant physical modes in the solution. The meshing software STAR CCM+ is used to develop a hybrid structured multi-block grid for meshing the computational domain which contain a total of 2148292 cells, 8802014 faces and 4838681 verts.

Figure 2.2 Smooth channel Mesh

Figure 2.3 Protruded channel mesh

Validation

Results validation is a very important step in any numerical study in order to ensure the numerical results are useable and it is ready for runs. The mesh integrity tests are first carried out for 0.8, 1, 1.6, 2 and 2.4 million cells. The result or friction factors and Nusselt number at Re 7000 are noticed deviate to turn of 14, 12 and 11% for 0.8, 1, and 1.6 million cells while negligible variations are observed for 2 and 2.4 million cells (1 – 3 % variations). The friction factor value and Nusselt number obtained from the CFD data for the smooth channel is compared with results from Karma Nikuradse, Shah and London, Gnielinski and Dittus-Boelter equations. The percentage deviation of the values of the predicted Nusselts number and friction factor to the CFD data was found to give maximum error of ±5.8 % and ±6 % respectively. This shows a good agreement between the present study and previous study and establish accuracy of the CFD data.

Results and discussions

Simulations were carried out in STARCCM+ to study the effect of channel height and Reynolds number variation on heat transfer friction factors and performance of passive oval protruded geometry. The effect on heat transfer and fluid friction were evaluated in terms of the relative Nusselt number, relative friction factor and thermal performance.
The simulation of the protruded channel is compared with the smooth channel and validated numerically.

Numerical Result Analysis

The surface geometry was imported from Solidworks Rx 5015 into the commercial simulation STARCCM+. The computational analysis was carried out and results were acquired after a successful simulation process
The structured mesh system shown in Fig. 2.2 and 2.3 were generated from the commercial software STARCCM+ with a total cell of 2,000,000. And the meshes near the walls and test section domain were refined to ensure the y+ values near the walls were <1. The governing equations for the flow and heat transfer were solved by the STARCCM+.

Nusselt number

Pointwise Nusselt number

The Nusselt number represents the enhancement of heat transfer through a fluid layer as a result of convection relative to conduction across the same fluid layer. The larger the Nusselt number, the more effective the convection. The Nusselt number which is calculated using equation 4 from the temperature extracted on fifty points along the channel length is plotted against the distance to show the heat transfer at various point along the length of the channel at different Reynolds number. Figure 4.1, 4.2 and 4.3 shows the variation of the relative Nusselt number versus the Position of different Reynolds number on the test section of the channel of height of 5mm, 7mm and 10mm respectively.

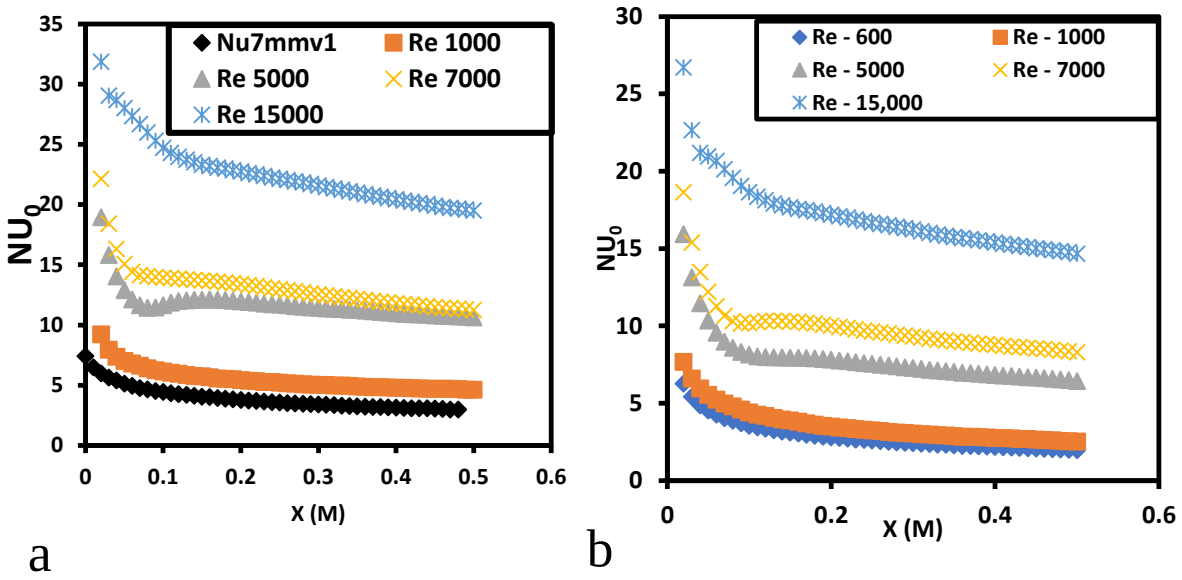

Figure 3.1 baseline Nusselt number for (a) H= 7 mm and (b) H = 10 mm

Figure 3.2: Contour along the smooth channel (H: 7mm and Re 5000)

For the channel with protrusion the thermal characteristics which is indicated by the Nusselt number across the direction of fluid flow (on the test section) having the same boundary condition as the smooth channel (baseline). The pointwise Nusselt number of different Reynolds number plot for the protruded channel is plotted in Figure 4.4 and 4.5

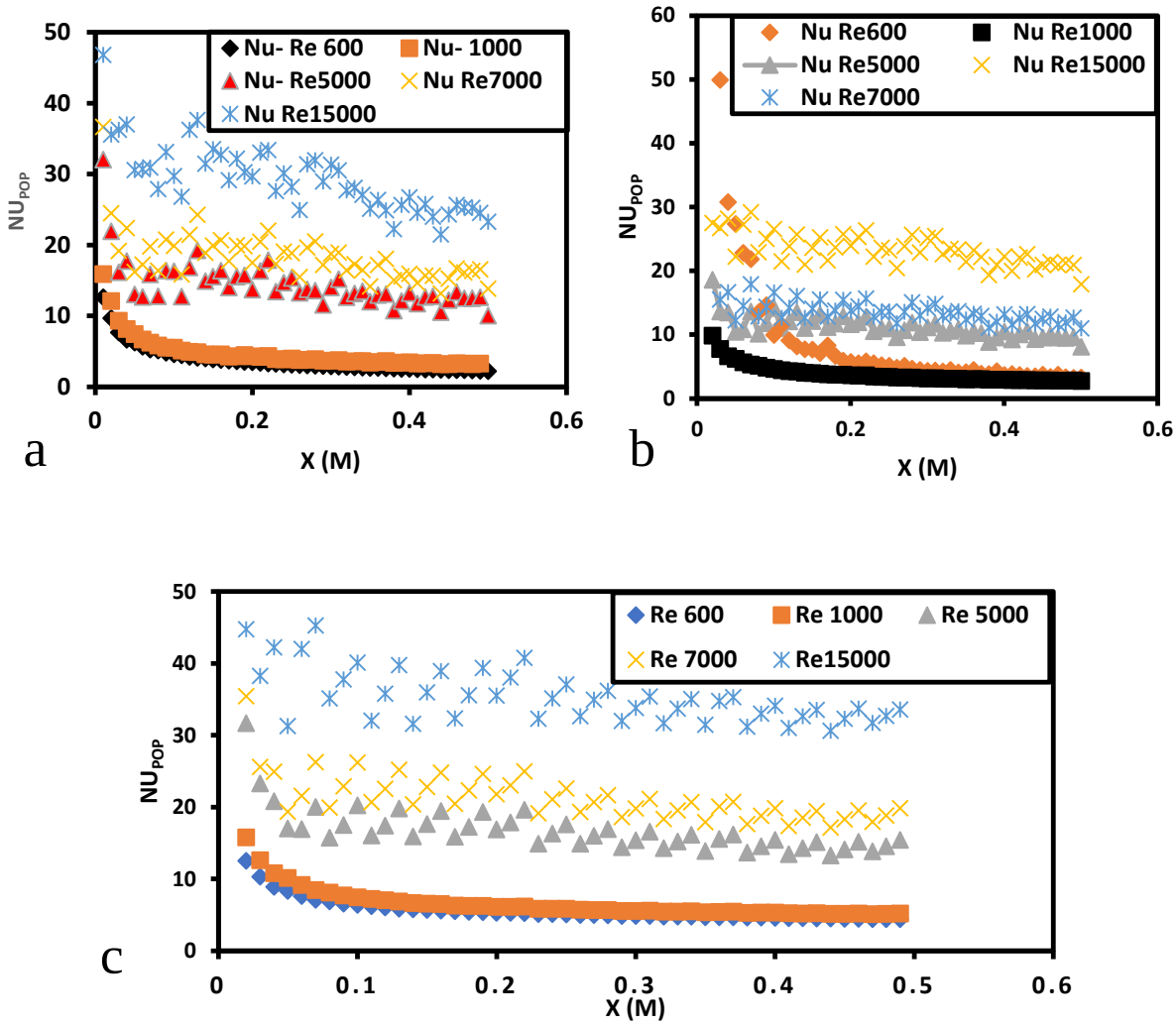

Figure 3.2 Mainstream Nusselt number for POP (a) 5 mm (b) H= 7 mm and (c) H = 10 mm

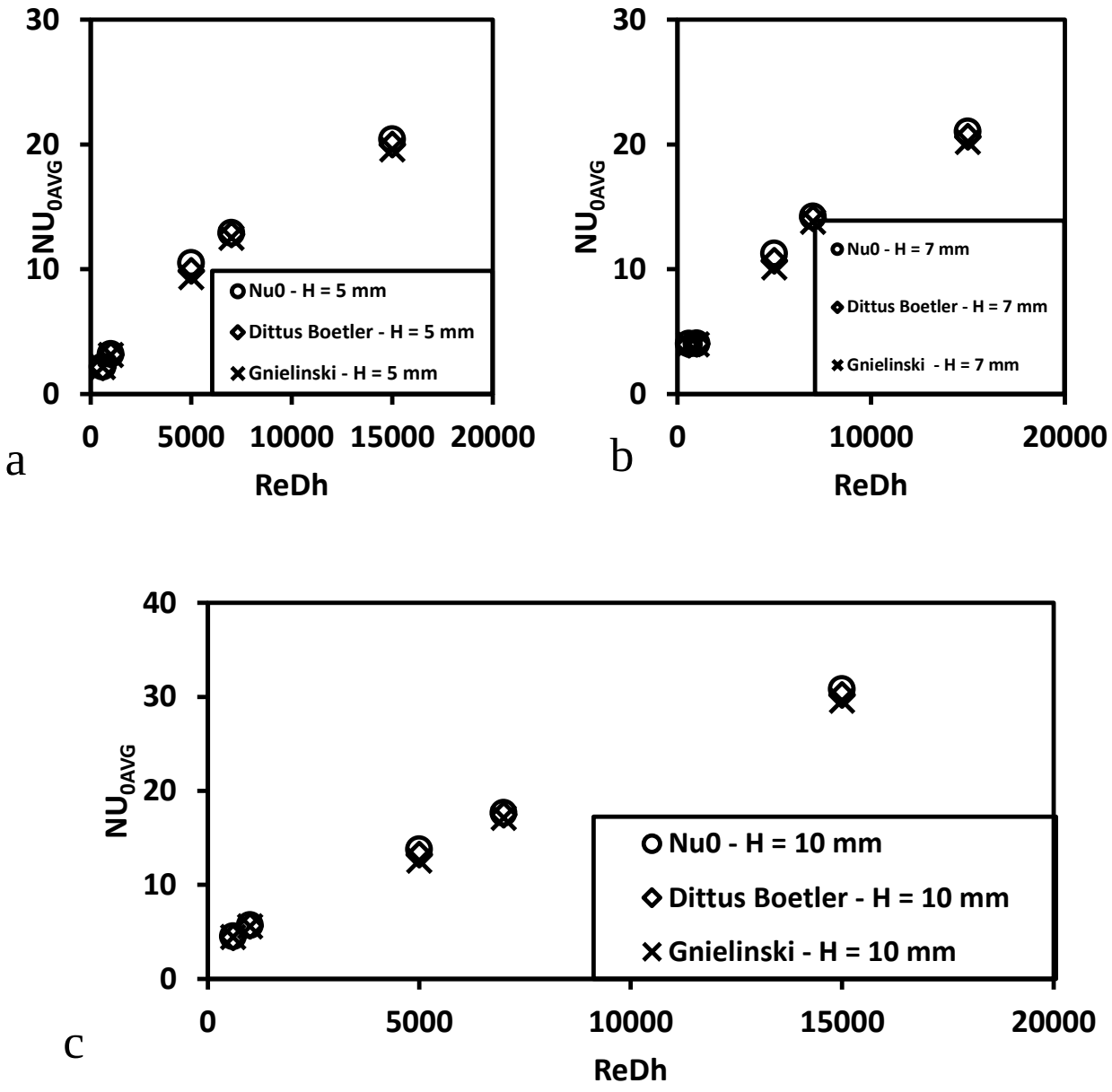

Figure 3.3: Validated averaged baseline Nusselt number for (a) 5 mm (b) H= 7 mm and (c) H = 10 mm

Average Nusselt number

The plot shows an increase in Nusselts number compare to smooth channel of the same channel height which implies a better heat transfer. The average Nusselt number (Nu_{av}) was computed and plot against Reynolds number to show the heat transfer performance for the smooth and roughened channel at different velocities.

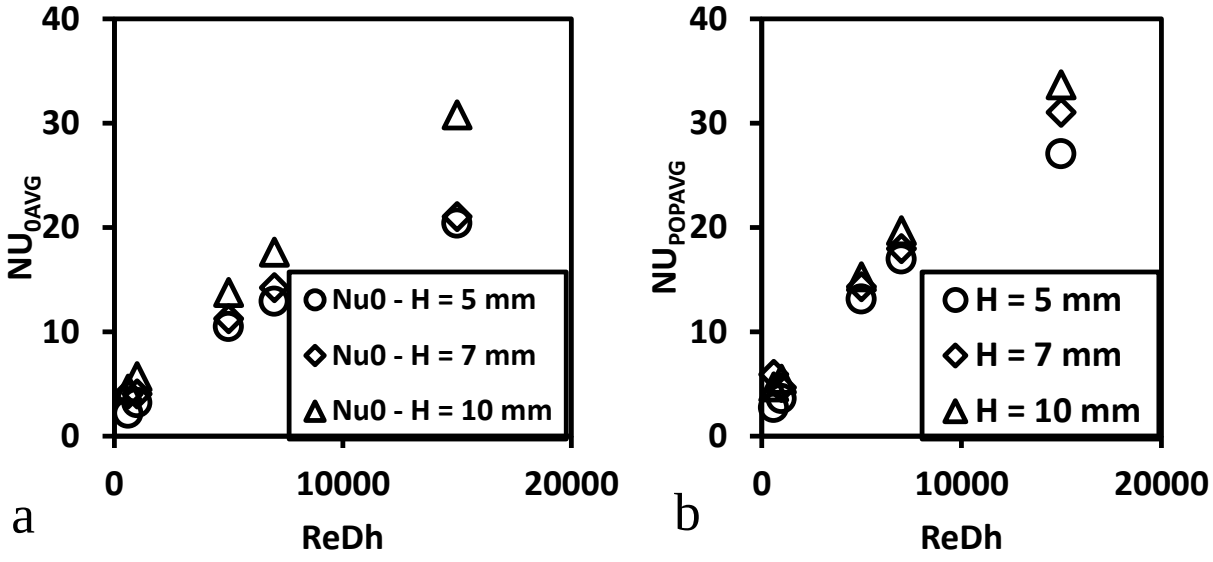

Figure 3.4 averaged Nusselt number for (a) Baseline (b) Passive oval protrusion, POP,

The plot for both the smooth and protruded channel shows that the channel with the channel height affect the Nusselt number at various Reynolds number of the flow. It can be seen that the protruded channel provides a higher Nusselt number than the smooth channel providing a better thermal transfer.

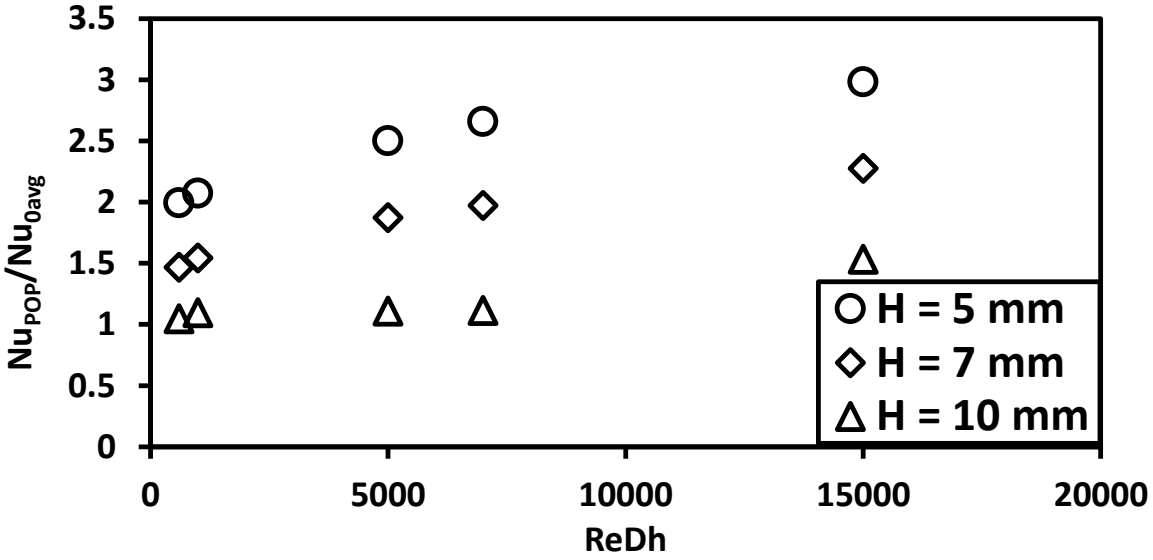

Figure 3.5: Normalised averaged Nusselt number

The ratio of the average Nusselt number of the roughened channel and smooth channel at different Reynolds number is plotted to predict the thermal performance at different channel height. The channel with height of 7mm shows the higher thermal performance among the three channel heights.

4.3. Pressure Drop

The static pressure along the channel was extracted from the simulation, the static pressure for roughened and smooth channel at channel height of 5mm, 7mm and 10mm.

4.3.1. Point-wise Static Pressure drop

The static pressure drops along the main stream (test section) of the rectangular channel for both the smooth and protruded channel was extracted from fifty points on the channel. The gradient of the graph of the static pressure against the distance of the extracted

point is the pressure difference (dp/dx). The plot figure 4.2 shows that the pressure drop decreases for all Reynolds number across the mainstream from the inlet to the outlet for both the smooth and roughened channel.

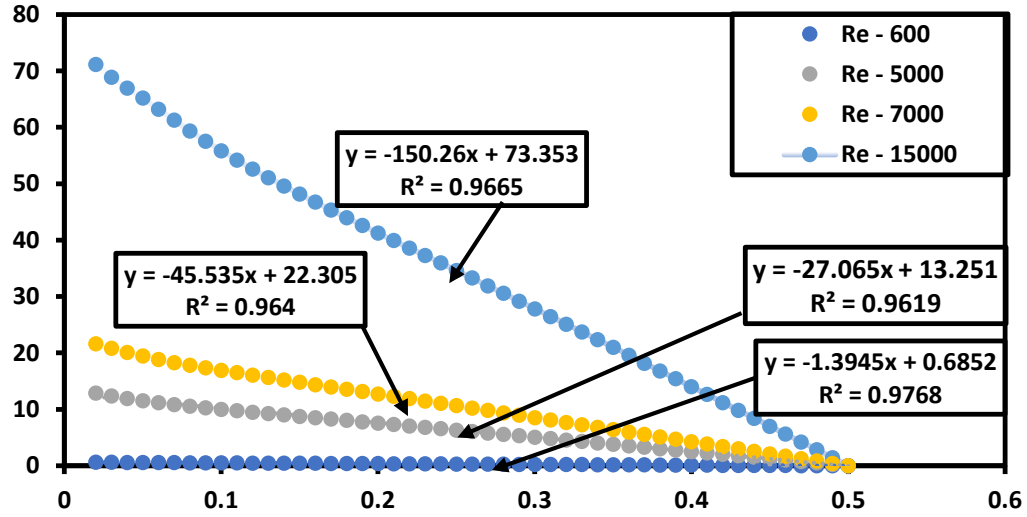

Figure 3.6: Pointwise static pressure along the mainstream of channel for 10 mm channel height

Figure 3.6 presents the static pressure drops along the mainstream of the channel. Static pressure drop shows how a surface influences the turbulation as a result of its degree of roughness. Having acquired this data a perfect line of fit is set on that and the coefficient, pressure drops, of which is used to evaluate the friction factor of the Reynolds number. From the acquired data same trend is observed for all cases in the smooth and protruded channel. The trends appear to decrease downstream of the channel making the pressure drop to negatives and creases as Re number changes. In general, the static pressure for all protruded channel is higher than the smooth channel static pressure of same Reynolds number and channel height.

4.3.2. Friction factor

The friction factor is used to determine the pressure drop which is calculated using equation 4. The friction parameter (dP/dx) is the gradient of the plot of the point-wise static pressure. Friction factor is plotted against the respective Reynolds number for both the smooth and protruded channel. Figure 4.5 shows the variation of the friction factor with Reynolds number for various height of the channel. It was observed from the plots that for both the smooth and roughened channel, the friction factor decreases as the Reynolds number increases.

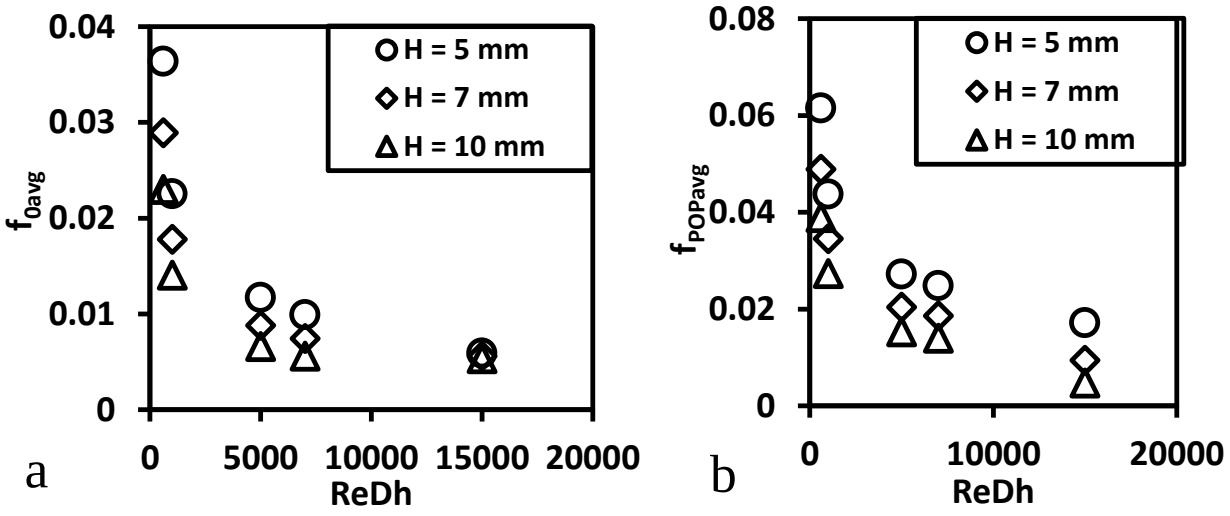

Figure 3.7: Averaged friction factor for (a) Baseline (b) Passive oval protrusion, POP

The friction factor ratio is the ratio of the average friction factor of the protruded channel to the average friction factor of the smooth channel (f_r/f_0). It also referred to as the normalized values of friction factor. The normalized friction factor (friction factor ratio) values obtained is plotted against its respective Reynolds number $600 \leq Re \leq 15000$.

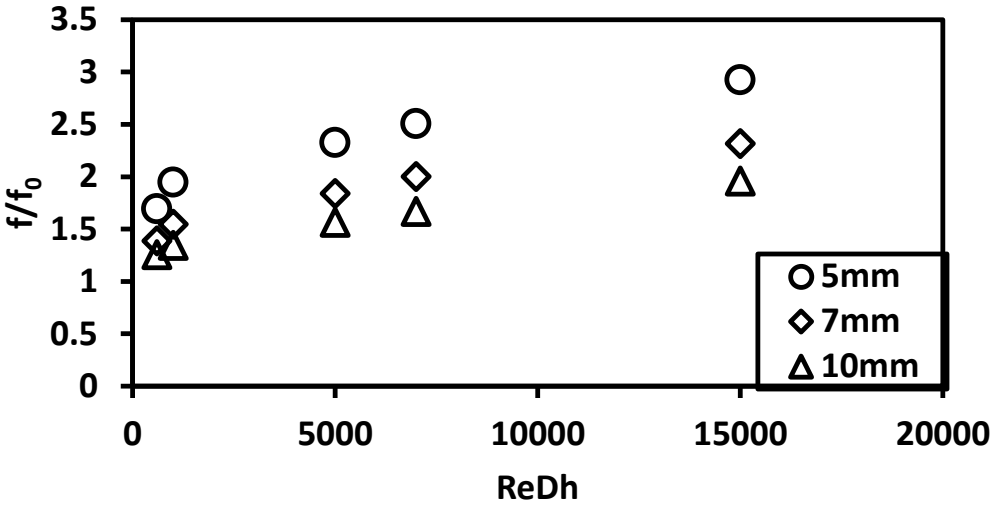

Figure 3.8: Normalised Averaged friction factor

The plot of the normalized friction factor to Reynolds number demonstrates an increase in normalized friction factor as the Reynolds number increases, and increasing the channel height decreases the normalized friction factor values.

Efficiency and Performance Index of the system

The performance index is the ratio of the normalized Nusselt number to the cube root of the normalized friction factor. It is important to compare the performance index with various Reynolds number.

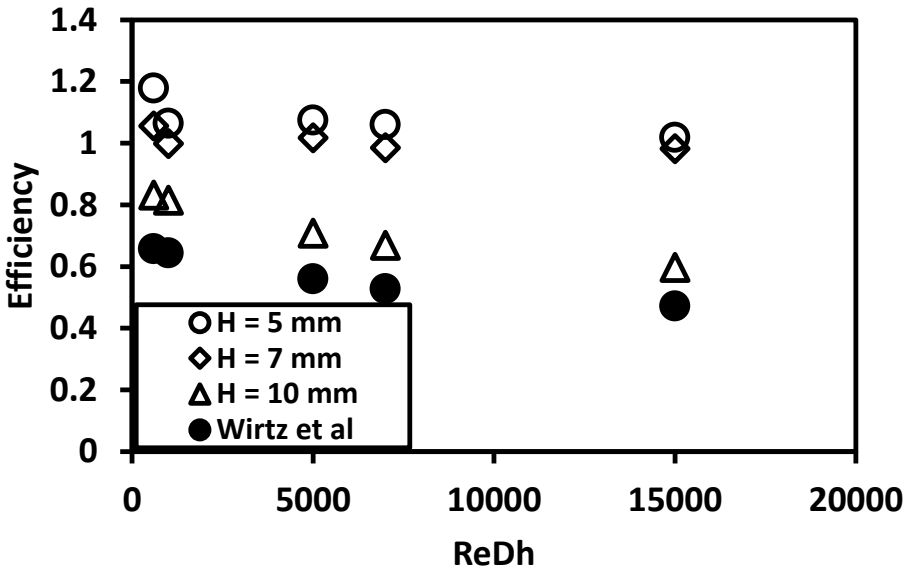

Figure 3.9: Performance efficiency of the system

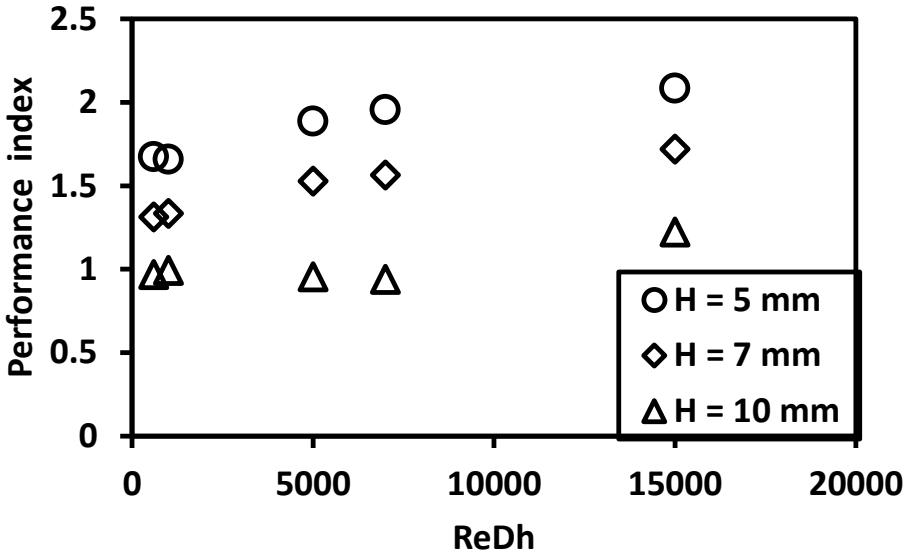

Figure 3.10: Performance index of the system

Figure 3.10 shows Performance index versus Reynolds number behaviour. Performance index increases with increase in Reynolds number. When the channel height is decreased from 10mm to 5mm, the performance index improves, indicating better heat transfer compared to increase in friction. However, the performance index decreases when the channel height is increased from 7 to 10mm.

Conclusion

Three-dimensional computational fluid dynamics simulations of flow and heat transfer in a rectangular channel with passive oval protrusion, POP, at different channel heights, H = 5, 7, 10 mm, were carried out. The thermal and hydraulic effect of passive oval protrusions in channel of different channel height were analysed and compared with the smooth channel results. The analysis was carried in flow for 600≤Re≤15000. The overall performance was analysed and evaluated based on various criteria. The following major conclusions can be drawn from this study.

- The performance of fluid flow in a rectangular channel can be greatly enhanced if the internal wall is protruded.
- It is also deduced that the performance index increases as the Reynolds number increases. However, the performance becomes steady as it near the peak value of the Reynolds number. The performance index along the channel for the three-channel height is greater than 1, meaning that the protrusion configuration performance exceeds that of the smooth channel.
- From the point-wise Nusselt number variation Nusselt number ratios, the values of the Nusselt number along the mainstream of flow channels for the roughened channel is higher than smooth channels which shows an increase in heat transfer in the protruded channel.
- Also, friction factors and friction factors ratio increase as Reynolds number increases. Influence of moderate pressure penalties brought about by elongation of reattachment time is another advantage.

Further research on degree of orientation and other protrusion arrangements are recommended to establish the optimal performance arrangements and angle for various protruded surface orientation. This ensure improve efficiency of heating system. More future need to be done on this geometry in its arrangement, pitch ratio, protrusion spacing with more time for running the simulation. Good computers like should be provided, which will make the analysis faster.

References

1. Gulave, J. S., and Desale, P. P. S., 2017, "Review of Heat Transfer Enhancement Techniques of W Ribs," **5**(5), pp. 2015–2018.
2. Chu, W., Tsai, M., and Jan, S., 2019, "CFD Analysis and Experimental Verification on a New Type of Air-Cooled Heat Sink for Reducing Maximum Junction Temperature," (xxxx).
3. Rao, Y., Chen, P., and Wan, C., 2016, "International Journal of Heat and Mass Transfer Experimental and Numerical Investigation of Impingement Heat Transfer on the Surface with Micro W-Shaped Ribs," **93**, pp. 683–694.
4. Luan, Y., Yang, L., Bu, S., Sun, T., Sun, H., and Zunino, P., 2019, "International Journal of Heat and Mass Transfer Effect of

Connecting Holes on Flow and Heat Transfer in a Two-Pass Channel with and without Rib Turbulators," **133**, pp. 80–95.
5. 2016, "CFD Analysis of Air and Steam in a Rectangular," (November).
6. Liu, J., Hussain, S., Wang, J., Wang, L., Xie, G., and Sundén, B., 2017, "Heat Transfer Enhancement and Turbulent Flow in a High Aspect Ratio Channel (4 : 1) with Ribs of Various Truncation Types and Arrangements."
7. Li, Y., Rao, Y., Wang, D., Zhang, P., and Wu, X., 2019, "International Journal of Heat and Mass Transfer Heat Transfer and Pressure Loss of Turbulent Flow in Channels with Miniature Structured Ribs on One Wall," **131**, pp. 584–593.
8. Prakash, C., and Saini, R. P., 2018, "Heat Transfer and Friction in Rectangular Solar Air Heater Duct Having Spherical and Inclined Rib Protrusions as Roughness on Absorber Plate," Exp. Heat Transf., **00**(00), pp. 1–19.
9. Thakur, S., and Thakur, N. S., 2020, "Environmental Effects Impact of Multi-Staggered Rib Parameters of the ' W ' Shaped Roughness on the Performance of a Solar Air Heater Channel," Energy Sources, Part A Recover. Util. Environ. Eff., **00**(00), pp. 1–20.
10. Eiamsa-ard, S., and Promvonge, P., 2009, "Thermal Characteristics of Turbulent Rib-Grooved Channel Fl Ows ☆," **36**, pp. 705–711.
11. Gupta, D., Solanki, S. C., and Saini, J. S., 1993, "HEAT A N D FLUID FLOW IN RECTANGULAR SOLAR AIR HEATER DUCTS HAVING TRANSVERSE RIB ROUGHNESS ON ABSORBER PLATES," **51**(1), pp. 31–37.
12. Bharadwaj, G., Kaushal, M., and Goel, V., "International Journal of Sustainable Heat Transfer and Friction Characteristics of an Equilateral Triangular Solar Air Heater Duct Using Inclined Continuous Ribs as Roughness Element on the Absorber Plate," (January 2014), pp. 37–41.
13. Angled, W., 2016, "Experimental Heat Transfer and Opposite Walls," **118**(January 1996).
14. Raghuraman, D. R. S., Karuppa, R. T., Nagarajan, P. K., and Rao, B. V. A., 2016, "Influence of Aspect Ratio on the Thermal Performance of Rectangular Shaped Micro Channel Heat Sink Using CFD Code," pp. 0–11.
15. Gawande, V. B., Dhoble, A. S., Zodpe, D. B., and Fale, S. G., 2018, "Thermal Performance Evaluation of Solar Air Heater Using Combined Square and Equilateral Triangular Rib Roughness," Aust. J. Mech. Eng., **00**(00), pp. 1–11.